

## Chapter 10

# 3-D modeling of the Southern Central Andes

This chapter describes the regional 3-D modeling developed to identify the principal conductivity structures of the forearc and arc of the Southern Central Andes, at latitudes between  $20^\circ$  and  $21.5^\circ\text{S}$  and longitudes  $68^\circ$  and  $70^\circ\text{W}$ . The MT data and the magnetic transfer functions have been considered for the fit the model responses.

The 3-D forward code of Mackie and Booker [1999] has been used for the computation of the model responses. The code is based on the original algorithm written by Mackie et al. [1994] which uses an integral form of Maxwell's equation to derive a finite difference approximation for the magnetic fields. The computing time of the algorithm strongly depends on the model grid definition (i.e., number of model parameters and cell spacing), which must be defined according to the conductivity variations and the penetration depths under consideration. On the other hand, the convergence of the EM-fields (based in an iterative finite difference approximation) will lose accuracy (and cost more time) the more irregular the grid is. A regular grid is ideal, but this can imply a high computing time by complicated and/or fine conductivity structures, for example, horizontal elongated conductors embedded in a much more resistive media, since the grid should be more finely defined at higher conductivity contrasts (Booker, pers.comm.). Thus, due to the small dimensions of the conductivity structures already identified by the qualitative 3-D modeling in the Coastal Cordillera and Precordillera (Chapters 7, 8), it is necessary to perform the quantitative 3-D modeling in two separate regions (Coastal Cordillera and Precordillera) in order to limit the number of parameters and hence reduce the calculating time, allowing an improvement on the forward approximation of the EM-fields as well. However, the degrees of freedom for each independent region are still large enough<sup>1</sup> to allow an optimal fit between model response and measured data, in contrast to what is usually achieved in 2-D inversion modeling cases. The computing time for a grid with dimensions  $95 \times 63 \times 43$  exceeds 12 hours, this means, each attempt costs more than 12 hours to improve the fit by means of trial and error testing. Due to the restrictions of the method affected by a high time consumption, the 3-D modeling should be considered

---

<sup>1</sup>Each region must consider the principal conductivity structures of its adjacent region to incorporate coupling effects

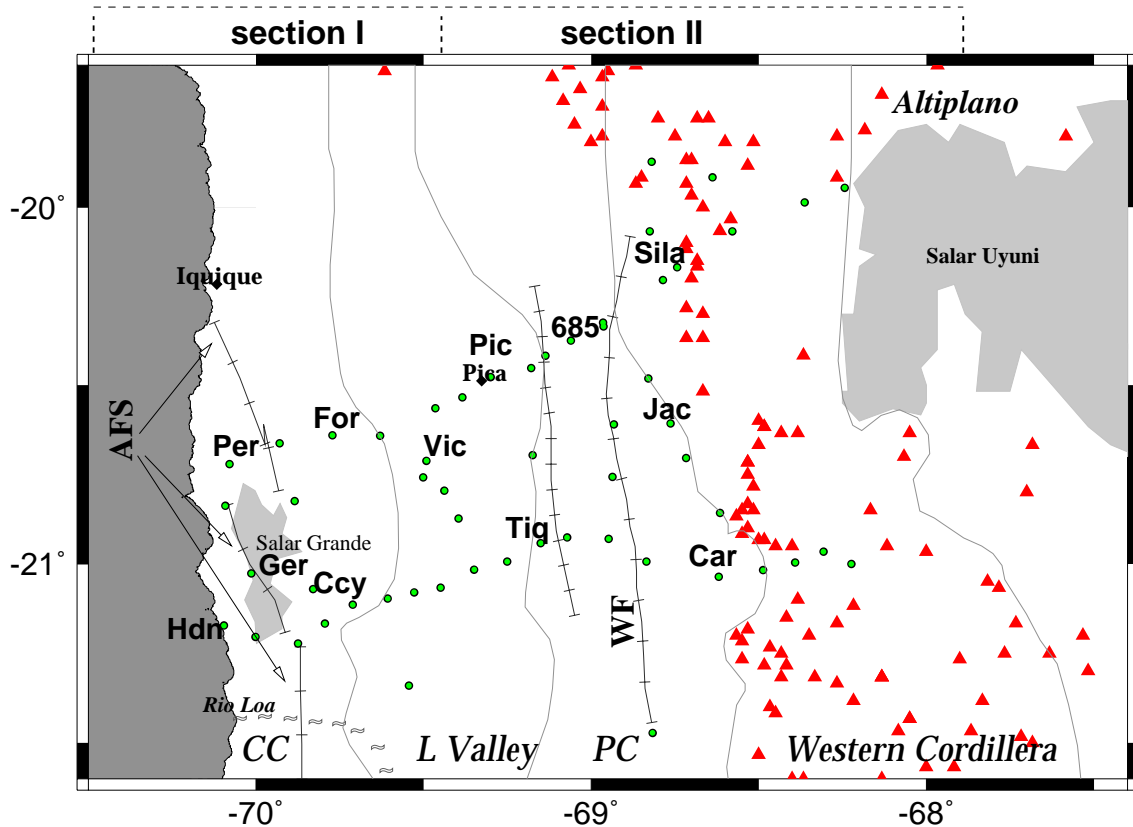


Figure 10.1: The study area for the 3-D modeling divided into two sections for the trial and error test. Section I, the Coastal Cordillera (CC) and Long Valley where the Atacama fault system (AFS) is located, with an active strike-slip motion in "Salar Grande". Section II comprises the L. Valley, Precordillera (PC), Western Cordillera (WC) and part of the Altiplano. The West Fissure (WF) is a regional strike-slip fault stretching along  $\sim$ N-S in the PC and continues still further south. Volcanoes of the magmatic arc are marked in red triangles. Green circles indicate the MT sites; labels are the treated for the comparison between the model response and data.

as connoisseur of the principal conductivity structures in the study area; higher conductivity complexities are out of scope.

As mentioned above, the 3-D structures considered in the forward modeling are known qualitatively from the analysis of current channeling (section 6.3), where near surface elongated conductors in the Coastal Cordillera (Chapter 7) and a 3-D anomaly in the Precordillera were identified (Chapter 8). Meanwhile the background 2-D conductivity values, particularly the deeper structures ( $>60$  km), are taken from the regional 2-D modeling (Chapter 9).

Alternative models are presented for the forearc region close to the coast (Coastal Cordillera) and the forearc-magmatic arc regions (Precordillera and Western Cordillera). In the near coast (fig.10.1; section I) are presented alternative geometries of conductive vertical dikes, associated with the Atacama Fault system (section 10.1).

The second region of the model study concentrates on the forearc-magmatic arc region (fig.10.1; section II), where the highly conductive features are a 3-D anomaly in the Precordillera (PC) and a HCZ beneath the Altiplano (section 10.2). The construction of the Precordillera anomaly (PC-conductor) itself was undertaken from the qualitative 3-D model interpretation of this region (section 8.2) and the 2-D forward modeling results (section 9.2).

The Altiplano high conductivity zone (AP-HCZ) was based on the 2-D inversion result, too (section 9.2). An alternative model is given by the connection between the PC-conductor and the AP-HCZ in the south (in section 10.2), motivated by the sensitivity analysis to 2-D structures after constraining a layer with a lower resistivity value in accordance with a low seismic velocity zone (section 9.2.3).

## 10.1 The Atacama fault zone

The modeling focuses on the near coast region (fig.10.1) and considers the Pacific Ocean, the Coastal Cordillera (CC), Long Valley and the Precordillera (PC). The Precordillera is included to compensate for coupling effects (see below). The features under consideration are the shallow horizontal elongated conductors in the Coastal Cordillera already identified qualitatively by the current channeling analysis (section 6.3). The conductors in the form of vertical dikes were inferred to strike in NNW-SSE direction (section 7).

The conductivity structure in the Precordillera affects the magnetic transfer functions of the near coast. This was inferred from the 2-D modeling (section 9.2), where an effect was observed at longer periods ( $>500$  s) given by the conductor in the Precordillera (PC-conductor) with its top boundary at 2 km depth (section 9.1.1). The long period induction arrows from the coastal sites thus require a conductivity zone in the Precordillera.

A 3-D structure in the Precordillera (PC;  $69^\circ\text{W}$ ) is placed at a depth below 10 km. This structure has been determined by trial and error in the modeling of the eastern sector (section 10.2), where shallower elongated conductors are additionally set beneath 2 km. For reasons of saving computing time, the shallower structure is not considered in this modeling section (this would have implied a finer grid discretization).

The PC-conductor has however little effect on the MT data of the Coastal Cordillera, where the ocean is seen to be the most prominent feature affecting the near coast region (section 9.1). This allows little attention to be paid to the continental conductivity structures further inland when explaining the MT data from the Coastal Cordillera.

Having established the ocean and the Precordillera conductor in the 3-D model, the elongated vertical dike-like conductors in the near coast have been determined by modeled trial and error, comparing the induction arrows of the data and model response. The conductors ( $5\text{-}10 \Omega\text{m}$ ) follow the trends of the Atacama faults (fig.10.2a) and are of limited horizontal extensions (8 km width,  $\sim 100$  km long), although their extension to the south cannot be discarded. Their southern continuation can not be resolved by the present MT site distribution. They are placed at shallow depths (200 m) extending down to 7 km, embedded in a  $200 \Omega\text{m}$  space. The resistivities are set to higher values ( $> 1000 \Omega\text{m}$ ) at depth over 15 km (fig.10.2c), similar as in the 2-D models (Chapter 9).

A discussion of the models is contained in a subsequent section (10.3).

### Induction arrows of the Coastal Cordillera

The induction arrows of the model response show a good fit with the data at short periods

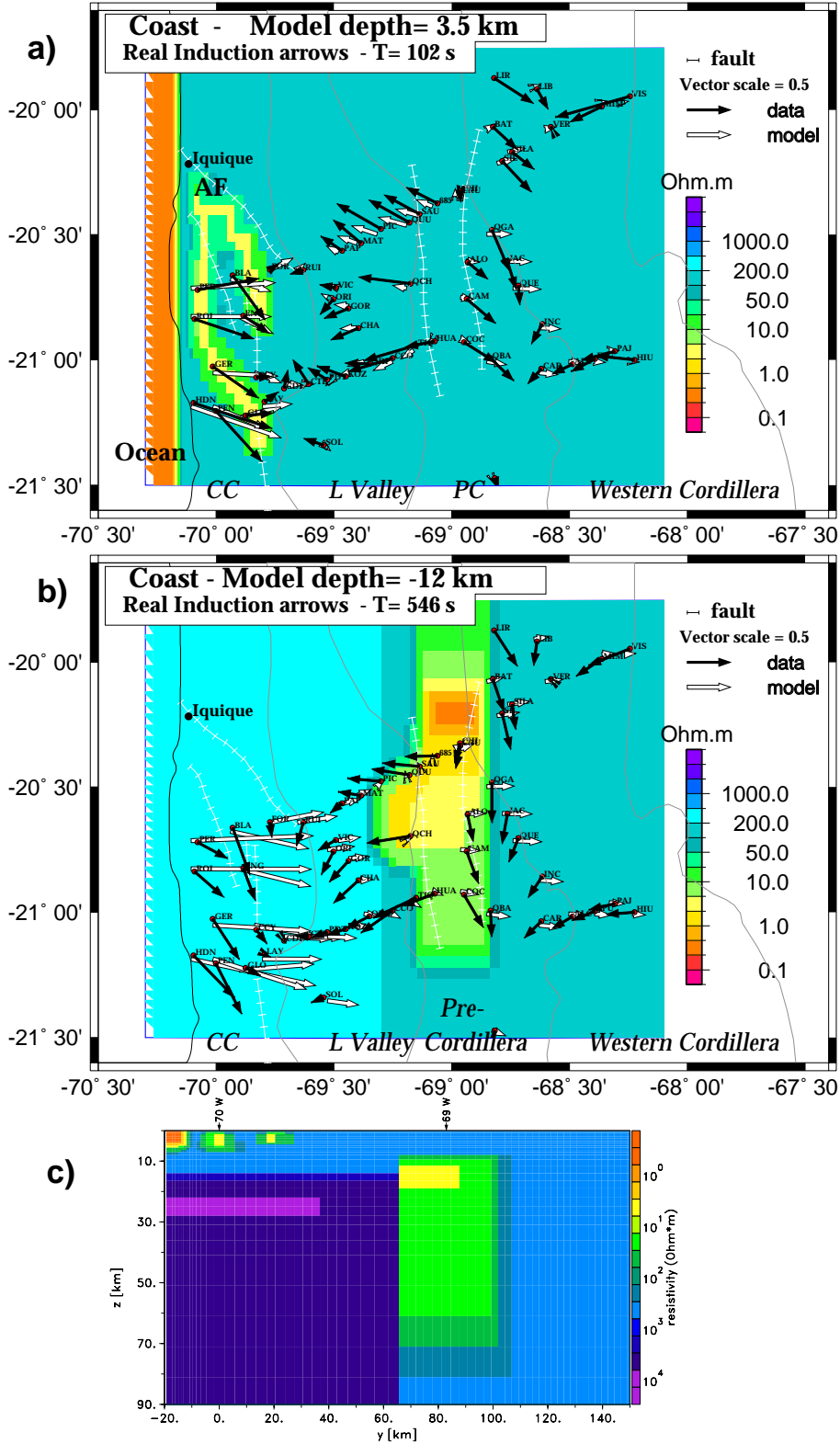


Figure 10.2:  
3-D model of the forearc region, to explain the data from the Coastal Cordillera (CC) where the Atacama fault (AF) is located.  
a) Horizontal view of the model at 3.5 km depth, projected on a geographical map with geological units. Included are induction arrows of the data (black) and the model response (white) at period 100 s.  
b) As in a) but here: model at 12 km depth and induction arrows at period 550 s.  
c) Vertical W-E cross section of the model at latitude 20.6°S.

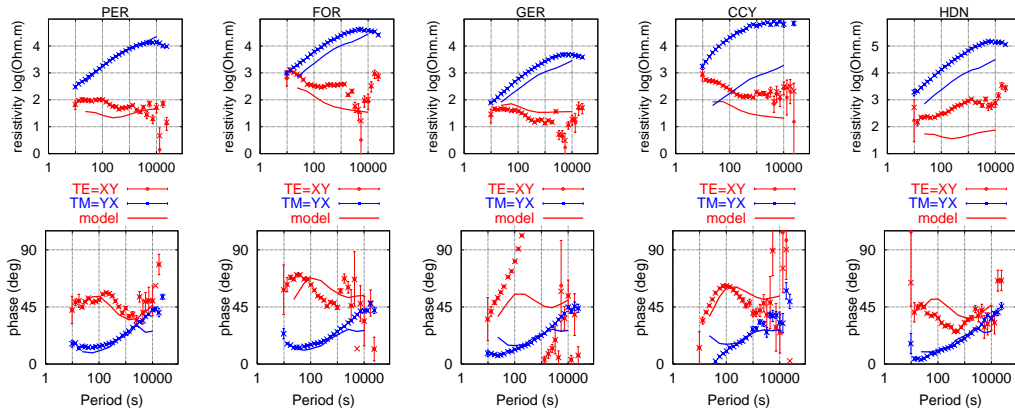


Figure 10.3: MT apparent resistivity and phases of the responses (lines) of the model shown in fig.10.2 compared with the data (points) for five sites distributed along the Atacama fault system. X is the geomagnetic north component.

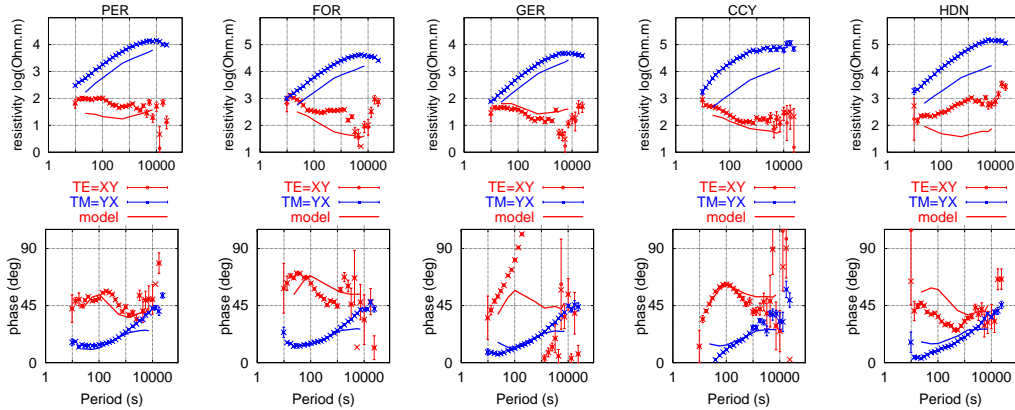


Figure 10.4: As in fig.10.3, comparison between data (points) and responses of the model (lines) shown in fig.10.5. X is the geomagnetic north component.

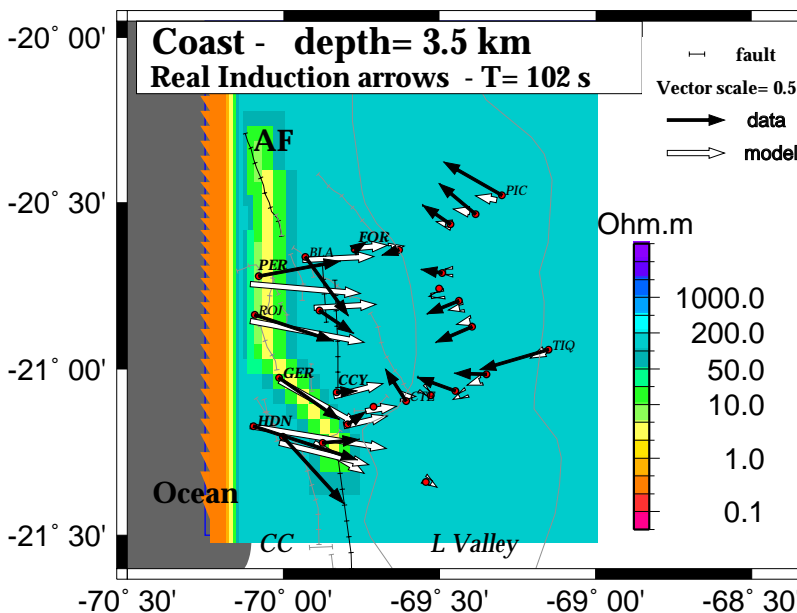


Figure 10.5: Horizontal view of an alternative model for the Atacama fault system (AF) projected at 3.5 km depth on the geographical map within the geological units. The MT sites show the induction arrows of the data (black) and the model response (white) at period 100 s.

(fig.10.2a), but the misfit increases at longer periods (fig.10.2b). The long period induction arrows of the model point to the east (i.e., they are affected mostly by the ocean), while the data vectors still point S-E. If the depth of the conductive dikes and/or the conductivity contrast between them and the host are not the reason for the misfit at long periods, it can be presumed that the PC conductor (69°W) needs to have higher conductances and should start at shallower depth as suggested by the model, in order to compensate for the strong ocean effect. Another (or additional) reason could be that the conductance of the ocean in the model has been overestimated, since it does not simulate the bathymetry of the Pacific but rather of a rough block of 4 km depth. Unfortunately, introducing such refinements to the model would cost even more time for the forward algorithm and would lead to worse accuracy in the EM-field approximation.

### MT Impedance tensor

Fit with the MT data is shown in fig.10.3 for five sites distributed along the Atacama fault system (see fig.10.5 for location). The fit for the TM-mode data is fairly good, while for the TE-mode data only some sites show a reasonable fit. The shift at the  $\rho_a$  curves between data and model response reflects an unresolved static shift effect<sup>2</sup>.

The anomalous current flow marked with magnetic distortion effects manifested in the TE-mode phases  $>90^\circ$  has not been reproduced by the model. This means the strong change in direction of the current flow produced by a coupling between the conductive dikes and the regional conductivity structure (section 7) does not occur in the model. In the model of section 10.3, it is shown that the current channeling effect is weak by the model responses, which is also marked with a negligible 3-D induction strength<sup>3</sup> in contradiction with the measured data (CC in fig.10.11a,b), although the depth of the dikes are defined greater in the next model (section 10.2). The crustal thin conductors in the Coastal Cordillera should have higher conductivity values (or the host can be set to lower resistivities) and/or are required to be larger in length, according to the current channeling hypothesis (section 6). However, the conductivity contrast has not been modified in the model since the forward computation losses accuracy by sharp conductivity contrasts unless the dimension of the grid is not finer defined.

### An alternative model

An alternative model has been tested (fig.10.5) which considers a simpler geometry for the elongated conductors. The fit of the induction arrows is partly improved to the south with regard to the the previous model, but they are worse to the north. The fit for the MT data (fig.10.4) is comparable with the previous model response (fig.10.3). The different shifts observed by the  $\rho_a$  curves between both model responses with regard to the data reflects that their difference of model structure is manifested mostly by a static shift effect, given the similar impedance phases that both have (figs. 10.3, 10.4).

---

<sup>2</sup>The static shift is produced by small local conductivity heterogeneities at the near surface.

<sup>3</sup>3-D induction strength is a measure of departure from the superposition model, i.e., a 2-D regional model superposed by shallow local 3-D structures, defined in section 6.1.8.

## 10.2 The Pre- and Western Cordillera

The modeling here focuses on the Precordillera (PC), the Western Cordillera (WC) and the most western part of the Altiplano (AP). The conductive ocean is however required by the TM-mode data and the long period induction arrows in these regions (section 9.1.1). Thus, the ocean and the near coast regions should be included in the model, too. The previous model was undertaken and the grid was refined and extended to the east for this model.

The conductivity structure in the Precordillera (PC) considers a conductor starting at shallow depth ( $> 2$  km; fig.10.7;  $69^\circ\text{W}$ ), as was inferred in section 8.2 to explain the intensity of the anomalous magnetic field observed in the data at short periods from this region (seen in the induction arrows and the magnetic distortion parameters of the superposition model), and later verified in the 2-D forward modeling for a vertical conductive block set between 2 and 10 km depth to explain the W-E components of the magnetic transfer functions (section 9.2).

From the current channeling analysis applied to the data of the Precordillera (PC), it is found that the model of local elongated conductors partially fits the MT data, whereas the 3-D induction strength is not negligible (Chapter 8). Assuming the presence of such elongated conductors and considering the sensitivity analysis of the data to the depth of the PC-conductor from the 2-D forward modeling (section 9.2), local vertical dike-like conductors of lateral finite extension are included in the model between 2 and 10 km depth with orientations near to the N-S strike and resistivities of 2-5  $\Omega\text{m}$  (fig.10.6a), following approximately the local azimuths indicated by the current channeling analysis (section 6.3.3).

According to the interpretation regarding a coupling effect between the shallow conductors and a deeper structure to explain the 3-D induction strength's increasing with period, a 3-D feature with similar geometry to that defined in the 3-D thin sheet modeling (section 8.2) is set beneath the shallow dikes ( $>10$  km depth). This same block was considered in the model of the previous section (fig.10.2b). The 3-D block has a gradual N-S resistivity variation of 2 to 50  $\Omega\text{m}$  from north to south, respectively, which has been determined by trial and error for the fit of the induction arrows at periods  $<1000$  s (fig.10.6b). The thickness of the block ( $>15$  km) has no influence in the magnetic transfer functions, as was found by the sensitivity analysis of the 2-D forward modeling (section 9.2). Through this 2-D modeling the horizontal components of the TM-mode fields (i.e., MT data) were seen to fit better the responses of the model for the block set at depth over 20 km (section 9.2), but at depths surpassing 30-35 km they are almost insensitive to a further increment of depth. Of course, this sensitivity analysis is restricted to a 2-D approximation, but under the limitations of the 3-D forward computation (a large number of model parameters) it is necessary to consider this result to constrain the degrees of freedom. The 3-D block in the Precordillera is set between 10 and 35 km depth. The whole PC-conductor is embedded in a 200  $\Omega\text{m}$  space (fig.10.7;  $69^\circ\text{W}$ ).

The largest high conductivity zone (HCZ) is in the east, between the Western Cordillera and the Altiplano, extending further to the east and hence into the Altiplano as a boundary condition. Its top layer is set at 15-20 km depth (fig.10.6b), with the highest conductivities ( $<2$   $\Omega\text{m}$ ) between 30 and 50 km (fig.10.6c), as in the 2-D inversion model of the Ancorp profile (section 9.2). This deeper HCZ bends in the NNW-SSE direction north of latitude  $21^\circ\text{S}$ . This bend –which follows similarly the geological limit trend– has been determined by trial and error for the fit of the induction arrows at long periods from the Pre- and

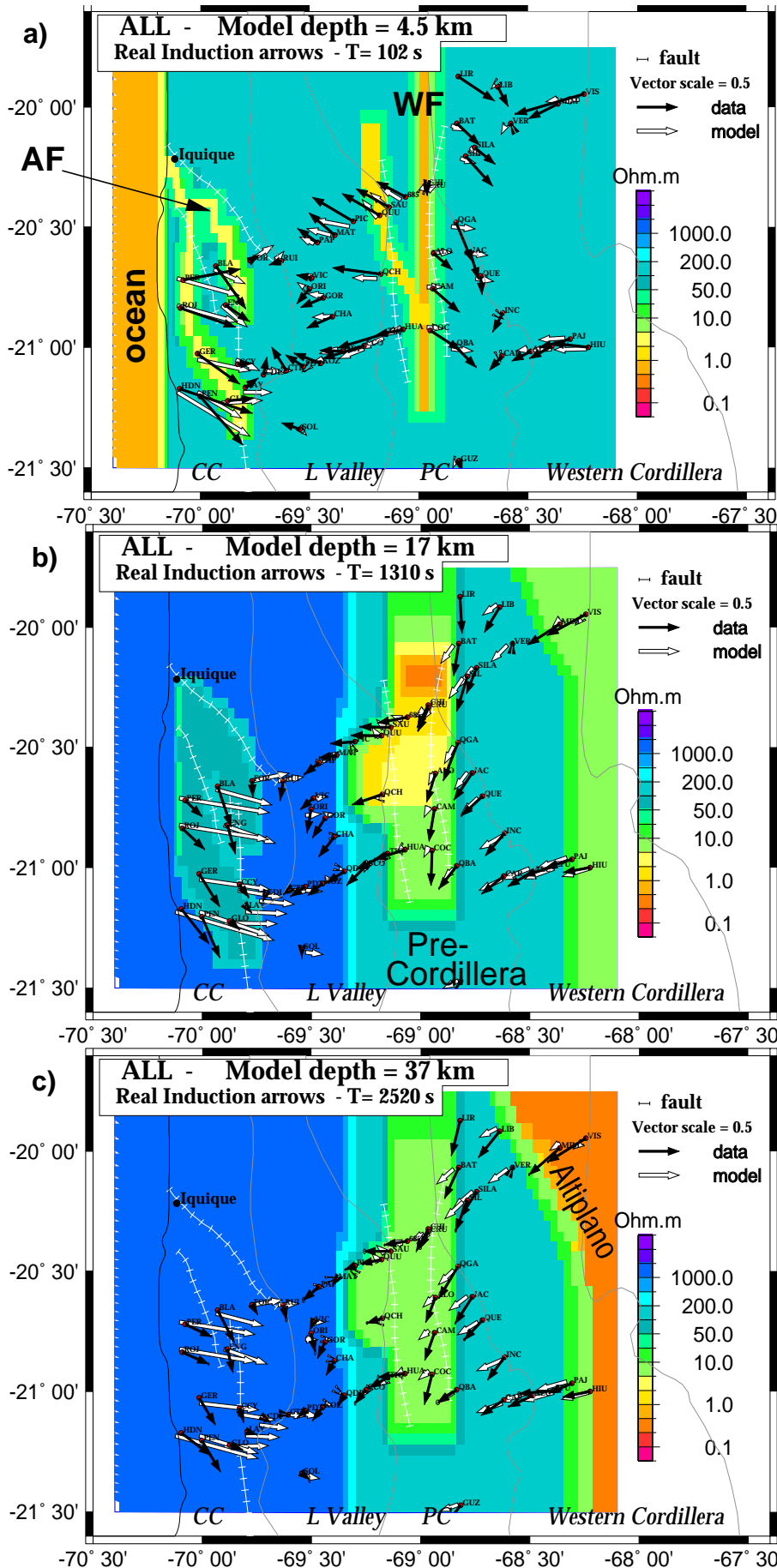


Figure 10.6: Horizontal views of the 3-D model at three different depths for the forearc (CC, L.Valley and PC) and magmatic arc (Western Cordillera) regions. Included are real induction arrows of the model response (white) and data (black) for periods representing corresponding penetration depths. The model is projected on a geographical map with tectonic units (AF, WF: Atacama fault and West Fissure).

a) Model at 4.5 km depth, and the induction arrows of period 100 s. b) Model at 17 km depth and the induction arrows of period 1300 s. c) Model at 37 km depth and the induction arrows of period 2500 s.



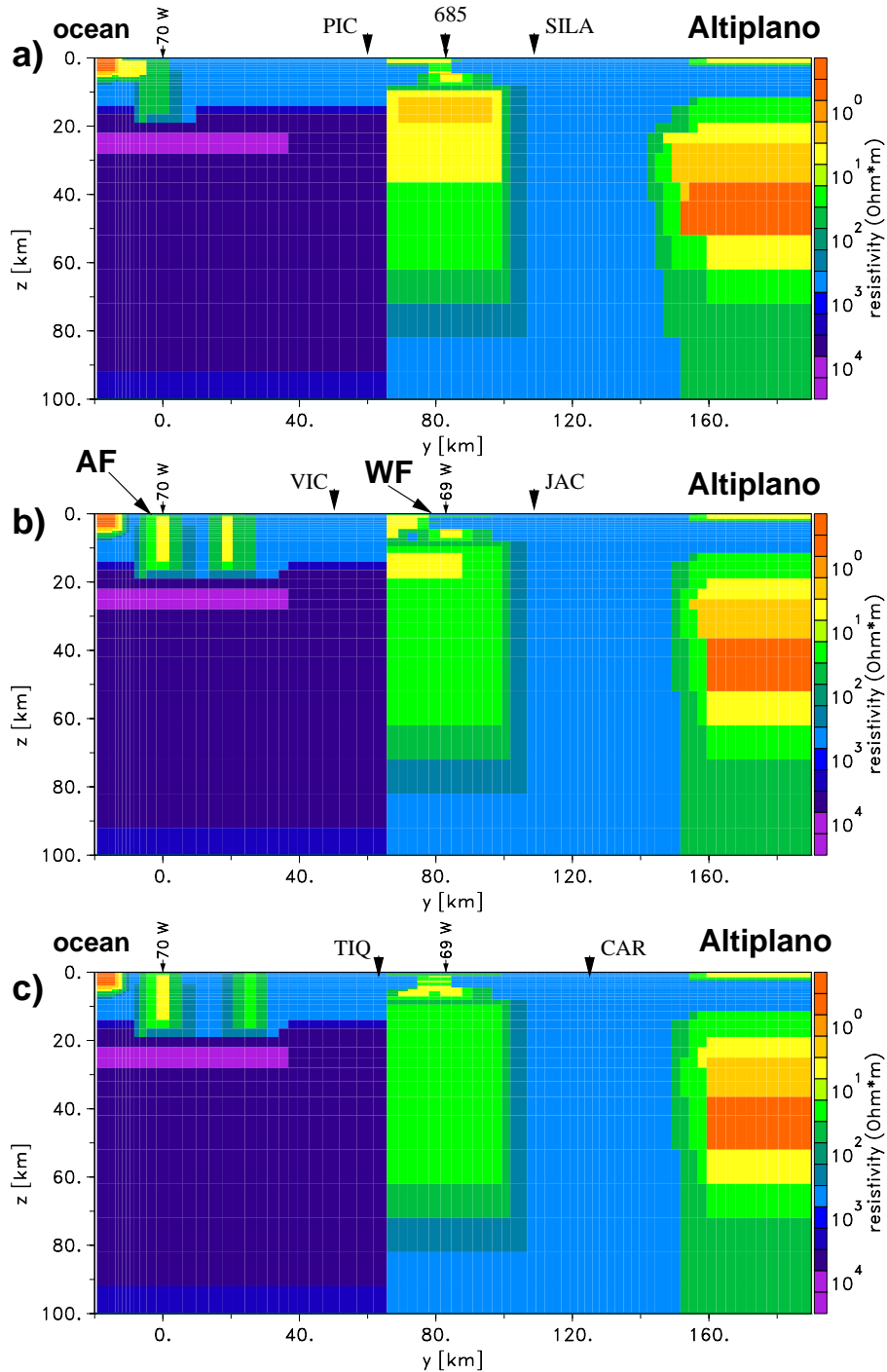


Figure 10.7: Vertical W-E cross sections of the 3-D model (fig.10.6) at latitudes 20.4°S (a), 20.7°S (b) and 21°S (c). The MT sites projected at the different sections are used for a comparison of the responses with an alternative model (fig.10.9). *AF*: Atacama fault, *WF*: West Fissure.

Western-Cordillera (fig.10.6c). Also, a shallow high conductive layer of 2 km thickness has been included, correlating with the thick sedimentary layer of the Altiplano (fig.10.7; right). The conductive dikes in the Coastal Cordillera have been extended vertically to a depth of 18 km, but this is seen to have little influence on the responses in the Precordillera and east of it. The model is shown in fig.10.6 (section 10.3).

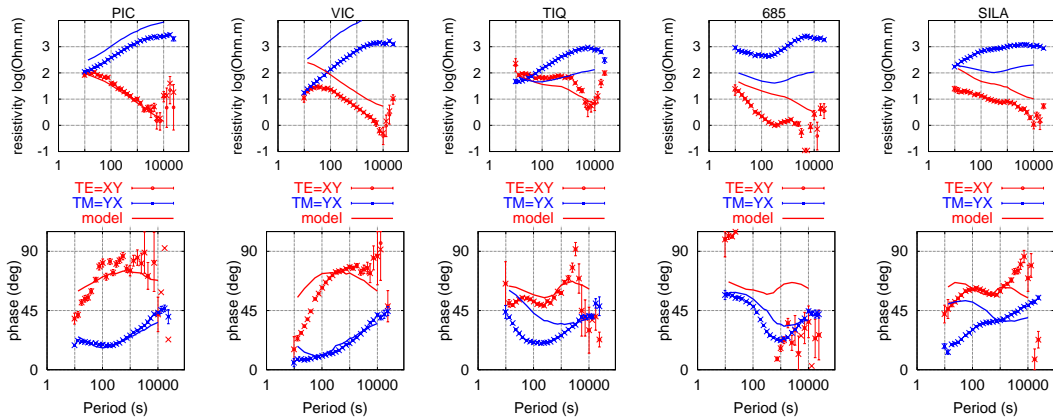


Figure 10.8: MT apparent resistivity and phases of the model response (lines) as compared to the data (points) for five sites distributed around the Precordillera fault system ( $69^{\circ}\text{W}$ ; model in fig.10.7). X is the geomagnetic north component.

The vertical cross sections of this model along the Pica ( $20.5^{\circ}\text{S}$ ) and Ancorp ( $21^{\circ}\text{S}$ ) profiles, and across an intermediate W-E profile, are displayed in fig.10.7.

### Induction arrows

At short periods, the induction arrows of the model response are smaller than the observed data in the Precordillera (PC in fig.10.6a). Furthermore, the modeled induction arrows vanish in the Longitudinal Valley at mid periods, whereas the measured vectors point SW, away from the Precordillera anomaly (fig.10.6b). Both observations indicate that the PC conductor of the model has lower conductance values (integrated conductivity) than it would need to reproduce the anomalous magnetic field observed in the region. However, this seems not to be true at longer penetration depths, since the long period averaged magnetic parameter of the galvanic distortion hypothesis (i.e., a measure of the regional magnetic field deviations due to 3-D structures; section 6.3) are similar between model response and data in the Precordillera (fig.10.11c; light-grays). On the other hand, the ocean of the model may produce a very strong effect on the on-shore conductivity structures, leading to attenuate the magnetic fields produced by the continental conductors to the point where the horizontal magnetic field components annihilate each other and hence the induction arrows vanish. Such case is observed in the Longitudinal Valley and western PC especially at long periods (fig.10.6b,c). In addition, for long penetration depths (long periods) the ocean in the model is the main effect seen on the induction arrows of the near coast (fig.10.6c; long white arrows in CC), whereas the observed data are much smaller, reflecting that the modeled ocean is overestimated as compared to the true effect of the real ocean.

### MT impedance tensor

Fig.10.8 shows a comparison between the MT model responses and the measured data of both polarization modes. Five representative sites were selected, distributed around the PC conductor (sites shown in fig.10.7). A good fit is seen at sites to the north-west of the PC conductor (sites PIC, VIC) located in the Longitudinal Valley, especially in the TM-mode.

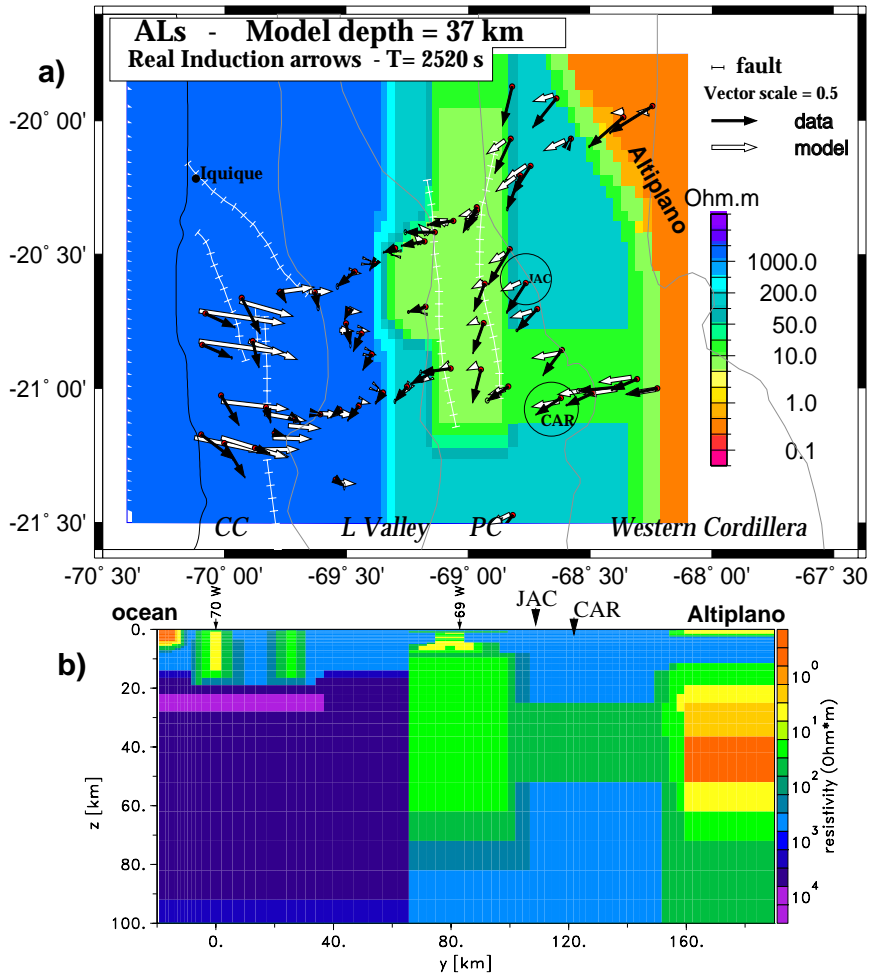


Figure 10.9: Alternative model with a low resistivity (20-50  $\Omega\text{m}$ ) layer connecting the Precordillera conductor (69°W) with the Altiplano (east) at latitude 21°S. a) Horizontal view of the model at 37 km depth. Real induction arrows of the model response (white) against the data (black) at period 2500 s. b) Vertical W-E cross sections of the 3-D model at latitude 21°S. The MT sites (JAC, CAR) projected at the profile are used to compare the responses with the other model (figs. 10.6, 10.7).

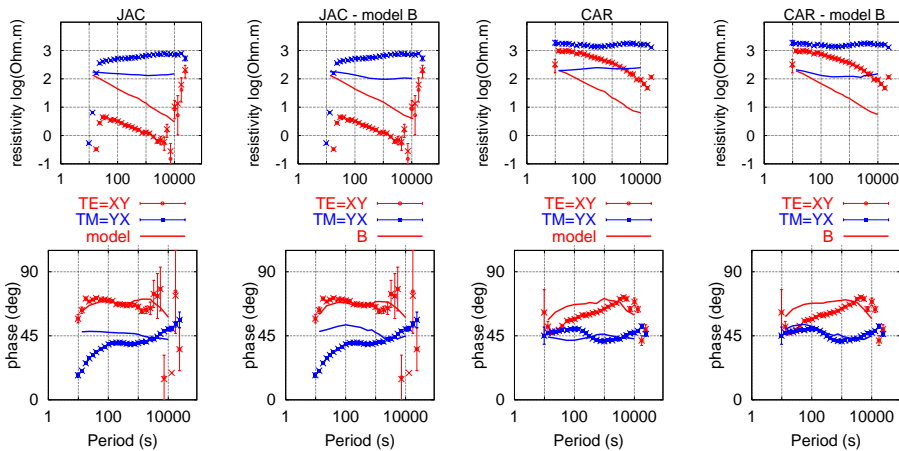


Figure 10.10: MT apparent resistivity and phases of the responses (lines) of the model shown in fig.10.7 and the alternative model B shown above against the data (points) for sites JAC and CAR. X is the geomagnetic north.

The parallel shift of the  $\rho_a$  curves reflects an unsolved static shift effect, while the TE-mode phase misfit reflects the magnetic distortion effect in the data at these locations (see next section). The misfit observed at the rest of the sites especially at short periods clearly indicates that a more complex conductivity structure at the near surface is present in the Precordillera as suggested by the 3-D model.

It also remains in question the sensitivity of the MT data to a variation in depth of the low resistivity ( $20 \Omega\text{m}$ ) bottom layer, which was set below 350 km depth beneath the Precordillera. In the qualitative 3-D thin sheet model interpretation of the Precordillera anomaly (section 8.2), a bottom conductive layer at shallower depth (100 km) was required to reproduce a similar magnetic distortion effect as is observed in the data, where TE-mode phases are sometimes  $>90^\circ$ . The data of site 685 are characterized by this strong distortion effect, while the response of the model treated here does not reproduce such an effect (fig.10.8; site 685). Adding a conductive layer at 100 km depth in the 3-D model would require a finer vertical grid discretization as well as a horizontal extension of the grid, demanding higher computing time.

### An alternative model

An alternative model was tested which differs from the former by a 20-50  $\Omega\text{m}$  layer at latitude  $21^\circ\text{S}$  (Ancorp profile). It was inserted between 25 and 50 km depth, connecting the PC conductor with the AP-HCZ (fig.10.9). The idea resulted from the 2-D modeling study (Section 9.2.3), where it was observed that such layer in the Ancorp model could improve the fit with TM-mode phases for sites above this structure, while this was not required further to the north (Pica profile at  $20.5^\circ\text{S}$ ).

The real induction arrows show slight differences from the former model in the region above the structure, as well as to the near north of it (figs. 10.6c and 10.9a, respectively). The misfit of the induction arrows actually increases for this alternative model.

Site CAR (Ancorp) of the alternative model located above the layer improves the fit with the TM-mode data (fig.10.10; CAR model B). The fit is however worse to the north of it (fig.10.10; site JAC), but is improved at the longest periods. In general, the fit of the MT data with this alternative model slightly improves with regard to the former model.

## 10.3 Discussion and outlook

A comparison of distortion parameters of the MT channeling analysis (3-D contour plots as in section 6.3.2) between model response and data is first shown in order to analyze dimensionality. The N-S conductivity variations of the model treated in section 10.2 (figs. 10.6, 10.7) are not as strong as those indicated by the measured data. This can be seen in the 3-D contour plot images of the long period 3-D induction strength parameter (fig.10.11b). This means the MT data are far from representing a two dimensional N-S striking superposition model almost everywhere (i.e., they suit a 3-D structure), whereas the model response indicates three dimensionality only in the Precordillera (PC) and east of the Western Cordillera (fig.10.11b; white). An induction effect marked with magnetic distortion is observed to be

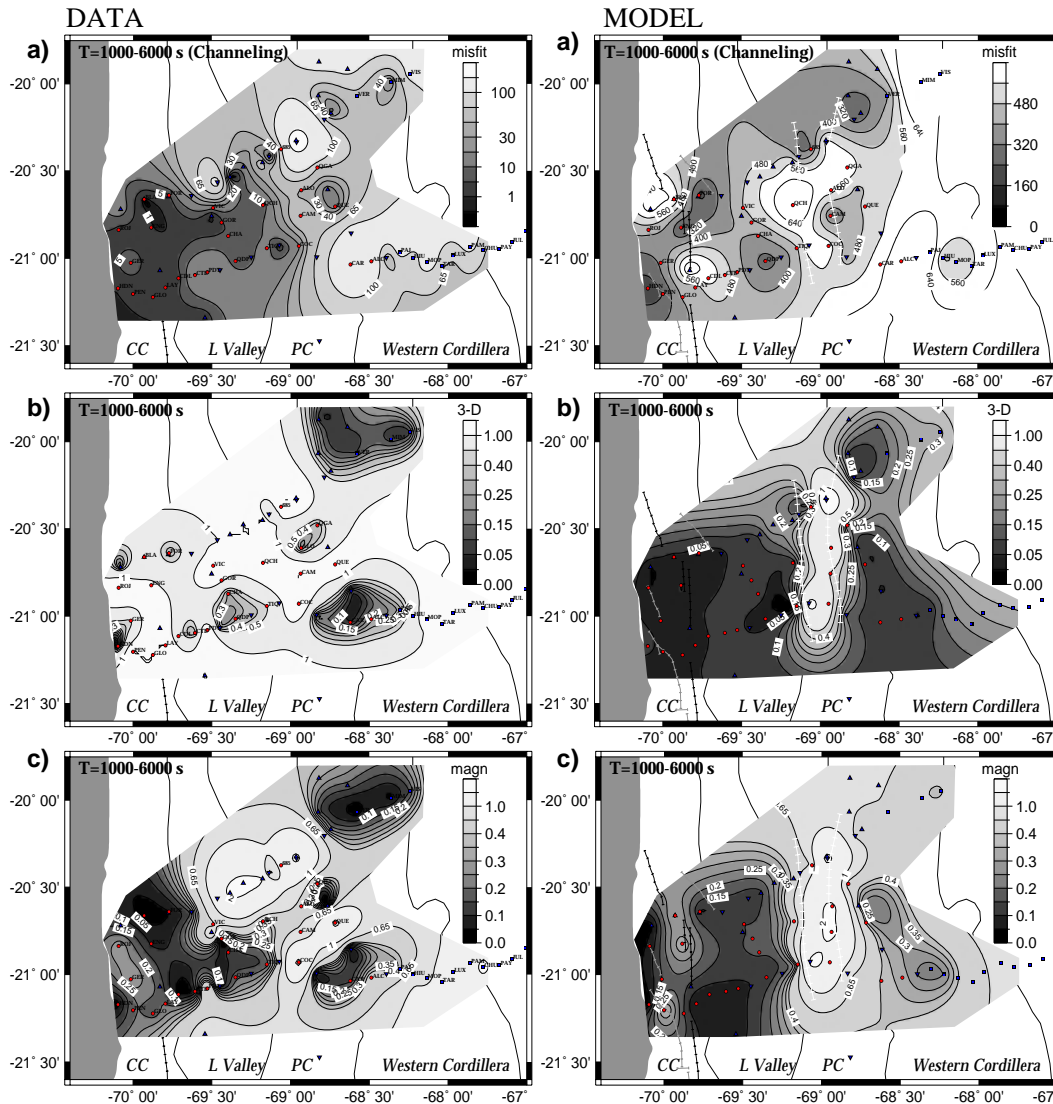


Figure 10.11: Interpolated site average parameters of the current channeling analysis (section 6.1) for the data (left) and the model responses (right). Procedure applied in the N-S coordinate system for the period band 1000-6000 s. a) Current channeling misfit. Light-grays indicate strong current channeling. b) 3-D induction strength, indicative of a 2-D superposition model departure (light-gray). c) Magnetic distortion, related to the deviation of the regional magnetic fields from the N-S coordinate system due to 3-D structures. Light-grays are associated to 3-D induction effects.

stronger in the data than in the model responses (fig.10.11c; white). This points to stronger N-S conductivity contrasts in the area than those considered in the model, which are beyond the limits of the 3-D forward computation for the grid defined in the modeling.

In the Coastal Cordillera (CC) and Long. Valley (LV), the current channeling effect seen in the model responses is too weak as compared to the data (fig.10.11a; light-gray), while the magnetic distortion (due to the elongated conductors) is comparable. The 3-D induction strength is however greater in the data (fig.10.11b; CC). The overestimated ocean of the model –a 2-D structure– might act as an attenuator of the 3-D induction effect in this region.

Altogether, it can be concluded that the strong distortion observed in the TE-polarisation

mode in the data (manifested sometimes by phases  $>90^\circ$ ) can not be reproduced by the model responses. This has also been observed in the Atacama fault model (CC) of the previous section (10.1). Since the TM-mode data are less distorted by the strong current channeling (sections 7, 8), a fit between these data sets and the corresponding 3-D model responses could be more realistic than in the TE-mode.

The models are discussed first for the Coastal Cordillera region and subsequently for the regions east of it, according to the conductivity structures characterizing the respective zones. In the Coastal Cordillera, the conductors can be linked with the Atacama fault. In the Precordillera, the conductor correlates with the Precordillera fault system (10.1).

#### **Atacama fault**

The vertical dike-like conductors down to a 7 km depth following the Atacama fault system can explain the induction arrows at short periods and the MT data in general (figs. 10.3, 10.4). A more complex geometry (fig.10.2a) or a simpler one (fig.10.5) are both alternative models for the Coastal Cordillera, since their responses are almost equivalent, differing principally by a static shift effect. The extension of the dikes to the north and south can not be determined by the present MT site distribution. The depth of the dikes are extended to about 20 km in the model of section 10.2 (fig.10.7; left), but their vertical prolongations nonetheless neither improve the fit for the induction arrows at longer periods nor achieve a comparable 3-D induction strength as observed by the MT measured data. Thus, the dikes extending in depth to either a 7 km or a 20 km (or even deeper), are alternative models for the region. This means the resolution in depth of the shallow dikes is not resolved. The fact that the strong current channeling effect observed in the data is not reproduced by the model responses is due to the conductivity contrast between the dikes and the host. A higher conductivity contrast is required in the model, and probably an ocean following the bathymetry of the Pacific as well, but this is beyond the limits of the forward computation for the given grid treated in the modeling.

#### **Precordillera and Western Cordillera**

A western extension of the Precordillera conductor in the direction of the Longitudinal Valley as expressed in the model (fig.10.6b;  $>10$  km) seems to be necessary to explain the induction arrows as well as the MT data (site PIC, VIC; fig.10.8). Also, the higher conductances to the north than to the south in the Precordillera are definitely required, considering the induction arrow data. The structures of the models have however a less significant N-S conductivity variation, as indicated by the 3-D induction strength parameter of the MT data (fig.10.11b), a difference which is based on the limitation of the forward computation by increasing the conductivity contrasts.

The evident N-S conductivity variation observed in the Precordillera seems to be linked with the different volcanic history known at these latitudes ( $21^\circ\text{S}$ ).

In the eastern Precordillera, it is not clear whether the layer connecting the Altiplano HCZ given in the alternative model at latitude  $21^\circ\text{S}$  (fig.10.9) is required. Actually, the eastern boundary of the Precordillera conductor has not been resolved properly by either model

(fig.10.7). Nevertheless, the NNW-SSE bend of the Altiplano HCZ (below 20 km depth) toward the Western Cordillera to the north can explain the SSW direction of the induction arrows at long periods (fig.10.6c).

Some questions remain in regard to structural changes that could be made to possibly improve the fit with the MT data, with the cost of a higher computing time, but time available for the elaboration of the thesis was limited. The modeling can be regarded as being at the stage where the principal 3-D structures have been certainly identified in the region.

One open question is namely the sensitivity of the data to the extension in depth of the conductors. For example, a further investigation should be made to scrutinize the requirement of a low resistivity bottom layer at a certain depth, particularly if a high conductivity zone above the oceanic slab beneath the Precordillera (PC) is required. Such a structure has been identified through the 2-D inversion modeling which gives an equivalent response to that of the model without it, but in the latter the PC conductor extends to greater depths (section 9.2.1). A similar 2-D model for the Pica profile (20.5°S) was obtained by Echternacht [1998], who argued that the MT data require a vertical PC-conductor split in two blocks separated by a 200  $\Omega\text{m}$  layer. The shallower block lies at depths between 5 and 30 km (2  $\Omega\text{m}$ ) and the deeper one beneath 60 km (0.5  $\Omega\text{m}$ ). Echternacht [1998] neither accounted for the magnetic transfer functions nor the three dimensionality. Nonetheless, it has been demonstrated here through a 3-D thin sheet modeling that a shallow 3-D conductive anomaly underlain by a deeper conductive layer ( $\sim 100$  km depth) reproduces the strong magnetic distortion manifested in the TE-mode impedance phases  $>90^\circ$  observed in the data (Chapter 8). This 3-D modeling supports the model obtained by Echternacht [1998] regarding the PC conductor split in two blocks and hence the idea of a shallow conductor related to the PC-faults and an additional conductive zone at the oceanic slab beneath the Precordillera.

In the 3-D models considered in this thesis, a 20  $\Omega\text{m}$  low resistivity layer was set at mantle depth (350 km), except beneath the Altiplano where the high conductivity zone (AP-HCZ;  $< 5 \Omega\text{m}$ ) below 20 km is connected with the low resistivity layer at 65 km depth (fig.10.7; right). The AP-HCZ follows approximately the resulting 2-d inversion models (section 9.2). Assuming that low resistivity values deep ( $>60$  km) beneath the Precordillera exist, one single low resistivity layer decreasing in value from west to east below the continental Moho (60-70 km depth; Chapter 3), correlating with a W-E increment of temperature from 400°C to 1250 °C (Springer and Förster [1998]), can be presumed to extend between the Precordillera and the Altiplano, thus constituting the wet mantle wedge.